Inorganica Chimica Acta 407 (2013) 210–215

Contents lists available at ScienceDirect

Inorganica Chimica Acta

journal homepage: www.elsevier.com/locate/ica

Solvent dependent mechanistic pathways for η-O_2CCH_3 substitution from the $[Mo_3(\mu_3\text{-}O)_2(\mu\text{-}O_2CCH_3)_6(\eta\text{-}O_2CCH_3)_3]^-$ anion

Jacqueline R. Houston *, Andrew J. Burton

Department of Chemistry, California State University, Sacramento, 6000 J Street, Sacramento, CA 95819, USA

ARTICLE INFO

Article history:
Received 2 July 2013
Received in revised form 29 July 2013
Accepted 30 July 2013
Available online 9 August 2013

Keywords:
Trinuclear molybdenum cluster
Kinetics
Ligand substitution
NMR
Solvent effects
Mechanism

ABSTRACT

Rate coefficients for terminal acetate (η-O_2CCH_3) substitution from the $[Mo_3(\mu_3\text{-}O)_2(\mu\text{-}O_2CCH_3)_6(\eta\text{-}O_2CCH_3)_3]^-$ anion were examined in polar protic (D_2O and methanol-d_4), polar aprotic (DMSO-d_6 and DMF-d_7) and acidic solvents (acetic acid-d_4). Reaction rates were determined using variable-temperature ^1H NMR and found to span orders of magnitude depending on the solvent ($k^{298\ K}$ (s^{-1}) = 7.2×10^{-6} for D_2O, 2.6×10^{-5} for methanol-d_4, 3.7×10^{-4} for acetic acid-d_4; no reaction for DMSO-d_6 and DMF-d_7). Unlike D_2O and methanol-d_4, little to no reaction occurs in DMSO-d_6 and DMF-d_7 most likely because the aprotic solvent is not able to solvate the leaving acetate ligand through hydrogen bonding. Activation parameters show that acetate substitution in polar protic solvents follows a dissociative pathway (D_2O: $\Delta H^{\ddagger}$ = 126 (±6) kJ mol^{-1} and $\Delta S^{\ddagger}$ = 80 (±18) J mol^{-1} K^{-1}; methanol-d_4: $\Delta H^{\ddagger}$ = 115 (±3) kJ mol^{-1} and $\Delta S^{\ddagger}$ = 52 (±9) J mol^{-1} K^{-1}) while parameters for acetate exchange in acetic acid-d_4 are markedly different and suggest a mechanism more complex than a simple ligand exchange reaction ($\Delta H^{\ddagger}_{obs}$ = 63 (±12) kJ mol^{-1} and $\Delta S^{\ddagger}_{obs}$ = −97 (±40) J mol^{-1} K^{-1}).

1. Introduction

Trinuclear molybdenum carboxylates, $[Mo_3(\mu_3\text{-}X)(\mu_3\text{-}Y)(\mu\text{-}O_2CR)_6L_3]^{z+}$(X = Y = O, X = Y = CR or X = O and Y = CR where R = CH_3 or another alkyl group and L = terminal ligand), have been examined for over three decades [1–6]. A typical synthesis involves refluxing $Mo(CO)_6$ in the presence of the corresponding carboxylic acid and anhydride to yield the bi-oxo capped cluster (X = Y = O) as well as some intriguing by-products such as the single-alkylidyne (X = O, Y = CR) and bi-alkylidyne capped clusters (X = Y = CR). Despite a comprehensive investigation on the synthesis of these complexes, only a handful of studies have examined the substitution reactivity of the terminal ligands. Of these studies, reports have shown that terminal ligand substitution follows a dissociative (D) or interchange-dissociative (I_D) pathway.

Most notable is the study by Powell and Richens which showed that aqua ligand exchange from the $[Mo_3(\mu_3\text{-}O)_2(\mu\text{-}O_2CCH_3)_6(H_2O)_3]^{2+}$ cation was relatively slow ($k^{298K} = 5.6 \times 10^{-6}$ s^{-1}) and that substitution was thought to occur through a dissociative mechanism [7]. As an extension to this work, Houston et al. later determined an activation volume for water substitution ($\Delta V^{\ddagger}$ = 8.1 cm^3 mol^{-1}) using high pressure ^{17}O NMR and confirmed the dissociative pathway originally proposed by Richens et al. [8]. Not only are dissociative mechanisms common for bi-oxo capped clusters, but also for related carbon-capped structures [9]. Given the structural data on molybdenum carboxylates, ligand substitution through a dissociative activation state is no surprise. Crystallography data shows that the Mo(IV) ion is 9-coordinate due to metal–metal bonding and that the average bond angle between the bridging carboxylate (μ-O_2CR, R = alkyl group) and the terminal ligand is roughly 75° [3–5,10]. As expected, crowding around the metal center would inhibit attack by an incoming ligand leading to a more dissociative activation pathway.

Herein we examine terminal acetate substitution at the $[Mo_3(\mu_3\text{-}O)_2(\mu\text{-}O_2CCH_3)_6(\eta\text{-}O_2CCH_3)_3]^-$ anion (abbreviated as **Mo_3**) by deuterated solvents (D_2O, methanol-d_4, DMSO-d_6, DMF-d_7 and acetic acid-d_4) using variable-temperature NMR (298–325 K). When the solvent is D_2O or methanol-d_4, we find that substitution follows the predicted D or I_D pathway based on highly positive activation parameters, yet in the presence of acid, parameters are distinctly different and suggest a mechanism more complex than a simple ligand exchange reaction.

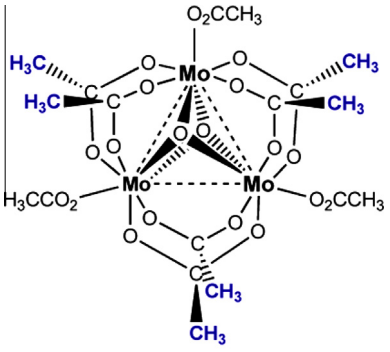

(Mo_3)

* Corresponding author. Tel.: +1 916 278 2583; fax: +1 916 278 4986.
E-mail address: jhouston@csus.edu (J.R. Houston).

0020-1693/$ - see front matter © 2013 Elsevier B.V. All rights reserved.
http://dx.doi.org/10.1016/j.ica.2013.07.054

2. Experimental methods

2.1. Materials and equipment

All reagents, solvents, and deuterated NMR solvents (D_2O (99.8%), methanol-d_4 (99.8%) acetic acid-d_4 (99.93%), DMSO-d_6 (99.9%), and DMF-d_7 (99.5%) were purchased from Sigma Aldrich. UV–Vis measurements were collected on a double-beam Shimadzu diode array system. ^{1}H and ^{13}C NMR spectra were collected on a 500 MHz Bruker Avance NMR. Magnetic measurements were done at room temperature using a Johnson Matthey magnetic susceptibility balance. Elemental Analysis was provided by Galbraith Laboratories.

2.2. Synthesis and characterization

The synthesis of $Na[Mo_3(\mu_3\text{-}O)_2(\mu\text{-}O_2CCH_3)_6(\eta\text{-}O_2CCH_3)_3]$ was first established by Cotton et al. (CAS 86695-77-4, Ref. [11]). Using a slightly modified procedure based on the experimental methods published by Noey et al. [12], 2.5 g of Na_2MoO_4 (12.1 mmol) was added to 3.0 g of $Mo(CO)_6$ (11.3 mmol) that had been dissolved in a mixture of acetic anhydride (100 mL) and acetic acid (10 mL). The solution was then refluxed at ~130–135 °C for 18 h (Caution: metal carbonyls evolve CO gas and are toxic). The blue-green reaction mixture was allowed to cool and then stand for 48 h. During this time, the solution turns a red-brown color and a red–orange solid slowly forms. The red solid was collected (yields range from 56–89%), filtered, washed with cold acetonitrile and ether, and dried under vacuum for characterization (^{1}H NMR, ^{13}C NMR, magnetic susceptibility, elemental analysis, and UV–Vis).

^{1}H NMR spectra were collected with 16 scans, a 90° pulse width of 11.50 μs and relaxation delay of 1.0 s on all samples. In D_2O, ^{1}H NMR assignments are as follows (δ in ppm, multiplicity, integration): 2.01, singlet, free-$O_2C\underline{\mathbf{C}}\mathbf{H_3}$ (when present); 2.16, singlet, 9H, η-$O_2C\underline{\mathbf{C}}\mathbf{H_3}$; 2.25, singlet, 18H, μ-$O_2C\underline{\mathbf{C}}\mathbf{H_3}$. ^{13}C NMR data were collected with 6,000 scans, pulse width of 9.25 μs and delay of 2.0 s (roughly 4 h run time). ^{13}C NMR assignments are as follows (δ in ppm, assignment): 21.49, free-$O_2C\underline{\mathbf{C}}H_3$ (when present); 22.56, η-$O_2C\underline{\mathbf{C}}H_3$; 24.63, μ-$O_2C\underline{\mathbf{C}}H_3$; 178.6, free-$O_2C\underline{\mathbf{C}}H_3$ (when present); 179.3, η-$O_2\underline{\mathbf{C}}CH_3$; 185.5, μ-$O_2\underline{\mathbf{C}}CH_3$. All chemical shifts are reported relative to TSP (^{1}H and ^{13}C NMR spectra are provided in the supplementary information, Supporting Figs. 1 and 2).

Microanalysis gave the expected stoichiometry. *Anal.* Calc. for $NaMo_3O_{20}C_{18}H_{27}\cdot 4H_2O$: Mo, 30.4; C, 22.8; H, 3.7. Found: Mo, 30.5; C, 21.9; H, 3.3%. Although the mass percents were slightly lower than calculated, the microanalysis data gave the expected Mo:C stoichiometry (Mo:C, 1.00:1.39 mass%) based on the formula above (Mo:C, 1.00:1.33). The electronic spectrum showed two broad absorption bands at 439 nm (ε = 509 L mol^{-1} cm^{-1}) and 518 nm (ε = 373 L mol^{-1} cm^{-1}) at a T = 295 K. Molar susceptibilities (X_m) were determined and shown to be small and negative (-2.97×10^{-4} to -4.63×10^{-4} cm^3 mol^{-1}), indicating that the compound is diamagnetic as expected due to metal–metal bonding.

2.3. Ligand substitution experiments using VT-NMR

An amount of 5 mg of sample was dissolved in 0.75 mL of D_2O ([**Mo$_3$**] = 7.0×10^{-4} M) containing a small amount of TSP for chemical shift referencing. Samples were chosen that contained little to no free acetate in order to quantitatively compare integrations. Once the temperature of the NMR probe reached 323.0 (±0.5) K, the sample was placed inside the spectrometer and allowed to equilibrate for several minutes. ^{1}H NMR spectra (16 scans) were then collected every 10 min for roughly 1.5–2 h. Reaction rates were examined by monitoring the signal intensity of the terminal acetate signal (I_t) as a function of time. To account for variations in signal intensity during data acquisition, all signal intensities were normalized to that of TSP. To determine a first-order rate constant, the ln(I_t) of the terminal acetate signal was plotted as a function of time. Activation parameters were calculated by monitoring the reaction at several temperatures (325.0, 323.0, 313.0 K, and room temperature). Substitution reactions were repeated using methanol-d_4, DMSO-d_6, DMF-d_7 and acetic acid-d_4.

3. Results and discussion

Rates and reaction pathways for acetate substitution are considerably affected by the nature of the solvent. When **Mo$_3$** is dissolved in a polar protic solvent such as D_2O or methanol-d_4, acetate substitution follows a dissociative (D or I_D) mechanism based on highly positive activation parameters. Shown in Fig. 1 are ^{1}H NMR spectra after **Mo$_3$** was dissolved in D_2O. Signals from the terminal (2.16 ppm, η-$O_2C\underline{\mathbf{C}}\mathbf{H_3}$) and bridging acetates (2.25 ppm, μ-$O_2C\underline{\mathbf{C}}\mathbf{H_3}$) are observed on the spectrum and the integrations correspond to a 1:2 ratio consistent with the stoichiometry (Fig. 1a; labeled t = 0, unreacted sample at room temperature). Upon heating at 323.0 K, the terminal acetate signal decreases due to substitution by D_2O and the bulk acetate signal appears on the spectrum (2.01 ppm, free-$O_2C\underline{\mathbf{C}}\mathbf{H_3}$). As expected, the integration of the terminal acetate signal equals the integration of the free acetate signal for all spectra collected, indicating that substitution is quantitative (the sum of the integrations remained constant over time, 2.13 arbitrary units (a.u.)). Also on the spectrum, we observe new signals from bridging acetates on substituted species (labeled b_m, b_d, and b_t for mono-, di- and tri-substituted complexes). The bridging acetate signal for the fully-substituted **Mo$_3$** complex appears at 2.20 ppm and the smaller signals are due to mono- and di-substituted species. Signals from substituted complexes are somewhat broad and found at slightly different chemical shifts than the unsubstituted trimer because the six bridging acetates are no longer chemically equivalent upon substitution. Loss of ideal D_3h symmetry results in two types of bridging acetates in a 1:2 ratio,

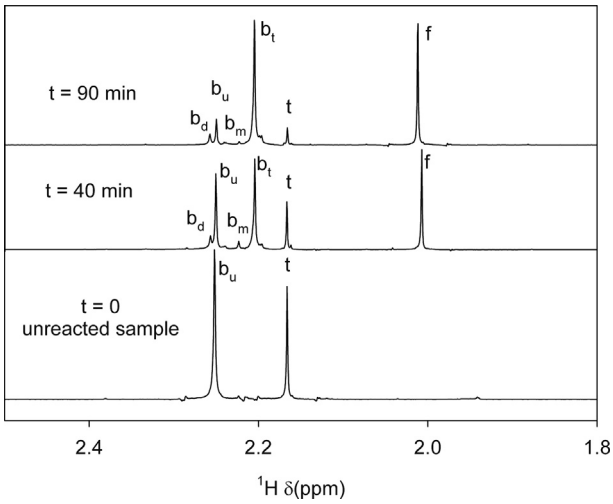

Fig. 1. ^{1}H NMR data for terminal acetate substitution by D_2O (T = 323.0 K). The disappearance of the terminal acetate peak (2.16 ppm, labeled t) is monitored over time. The integration for the terminal acetate signal equals the integration for the free acetate signal (2.01 ppm, labeled f), indicating that speciation is quantitative. Small signals emerge from the mono (2.22 ppm, b_m), di-(2.253 ppm, b_d) and trisubstituted species (2.20 ppm, b_t) and are tentatively assigned on the spectrum. The sum of the integrations for all substituted species during reaction (4.05 a.u) equals the integration for the unsubstituted signal at t = 0 (2.252 ppm, b_u, 3.98 a.u).

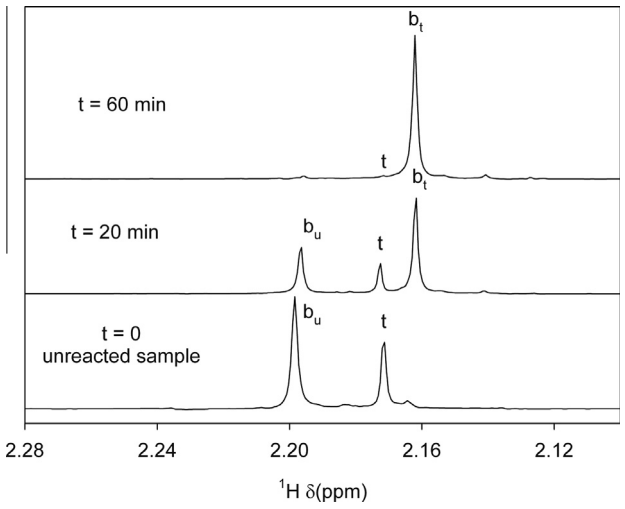

Fig. 2. ^{1}H NMR spectra for terminal acetate substitution by methanol-d_4 (T = 323.0 K). The disappearance of the terminal acetate peak (2.17 ppm, *t*) is monitored over time. The substitution reaction with methanol-d_4 is slightly faster (roughly a factor of three compared to D_2O) and signals from the intermediate species, the mono-, and di-substituted trimers are not observed. However, an NMR signal for the final product, the trisubstituted species is observed at 2.16 ppm (b_t). Free acetate at 1.95 ppm is not shown.

however this splitting is not well resolved in D_2O as it is for other solvents (e.g. acetic acid-d_4). Regardless, the ^{1}H NMR signal from the terminal acetate at 2.16 ppm is well resolved from the bridging signals and can be easily monitored over time.

Similar results were found when the **Mo$_3$** compound was dissolved in methanol-d_4 albeit the substitution reaction is slightly faster (Fig. 2). For this ligand substitution, signals from the intermediate mono- and di-substituted trimers are not observed. However, an NMR signal for the final product, the tri-substituted complex is observed at 2.16 ppm (labeled b_t). As expected, the integration of the unsubstituted bridging acetate signal (b_u, 1.07 a.u., 2.19 ppm) is equal to the integration for the trisubstituted species after reaction (b_t, 1.04 a.u, 2.16 ppm).

To determine a rate constant for substitution, the ^{1}H NMR signal from the terminal acetates was monitored for approximately three half lives and plotted as a function of time (Supporting Fig. 2).

$$\ln(I_t) = -k_{obs}t + \ln(I_o) \quad (1)$$

Eq. (1) is the integrated rate law used to analyze first-order reactions, where I_t represents the signal intensity at reaction time *t*, I_o is the initial intensity at $t = 0$ and k_{obs} is the observed rate constant. First-order kinetics applies in all cases because the substitution reaction is either dissociative (D_2O and methanol-d_4) in which rates do not depend on the incoming ligand or pseudo-first order in which the incoming ligand is the solvent (acetic acid-d_4) [13]. By monitoring the substitution reaction at several temperatures, an observed activation enthalpy ($\Delta H^‡$) and entropy ($\Delta S^‡$) were determined using the Eyring equation (Eq. (2)) [14].

$$k_{obs} = \frac{k_B T}{h} e^{-\left(\frac{\Delta H^‡ - T\Delta S^‡}{RT}\right)} \quad (2)$$

The term k_{obs} represents the rate coefficient for substitution, k_B is Boltzmann's constant, *T* is the experimental temperature in Kelvin, *h* is Planck's constant, and *R* is the gas constant. By plotting $\ln(k_{obs}/T)$ versus $1/T$, the $\Delta H^‡$ and $\Delta S^‡$ for substitution were determined to be 126 (±6) kJ mol^{-1} and 80 (±18) J mol^{-1} K^{-1} respectively, for reactions in D_2O. Activation parameters for substitution by methanol-d_4 were similar and determined to be $\Delta H^‡$ = 115 (±3) kJ mol^{-1} and $\Delta S^‡$ = 52 (±9) J mol^{-1} K^{-1}. Large positive activation parameters indicate a D or I_D pathway while a small $\Delta H^‡$ and negative $\Delta S^‡$ point towards an associative or bimolecular substitution. Our values for acetate substitution agree with aqua ligand exchange studies of molybdenum acetates [7–9], which suggests that regardless of the attached ligand, substitution reactions in polar protic solvents follow a dissociative mechanism (Table 1).

Interestingly, however, acetate substitution by polar aprotic solvents does not occur. Reactions run in DMSO-d_6 or DMF-d_7 show no evidence of reaction even at 323.0 K for over an hour (Fig. 3a and b). To induce reaction, a separate experiment was performed in which 250 μL of D_2O was injected into a sample containing 5 mg of **Mo$_3$** compound dissolved in 500 μL of DMSO-d_6 (Supporting Fig. 4). Evidence of substitution was clearly seen after 20 min (T = 323.0 K) unlike the experiment conducted in pure DMSO-d_6. Based on this data, we propose that acetate dissociation is facilitated by polar protic solvents that can stabilize the eliminated acetate ion through solvation. Because DMSO and DMF are not able to hydrogen bond to the leaving anion, little Mo-O(η-O_2CCH_3) bond polarization occurs prior to dissociation. As a result, rates are relatively slow.

Lastly, exchange of the terminal acetate ligands in acetic acid-d_4 (Scheme 1) was found to be two orders of magnitude faster than substitution by D_2O. Shown in Fig. 4 are ^{1}H NMR spectra immediately after mixing (top spectrum) and after the reaction is complete (bottom spectrum). On the initial spectrum, ligated acetates are assigned to the signal at 2.19 ppm (*t*) and signals further downfield at 2.20, 2.21 (split signal of 1:2 ratio), 2.25, and 2.32 ppm are assigned to unsubstituted (b_u), mono- (b_m), di- (b_d), and tri-substituted (b_t) species. Because the integrations of the substituted complexes cannot be quantitatively compared due to reaction and the chemical shifts are different than those found in D_2O due to solvent effects and pH [15], these assignments are based on chemical shift trends for well-established substituted molybdenum and rhodium trimers in acidic media [9,16]. The ^{1}H NMR spectrum after reaction (less than 30 min, T = 323.0 K) shows only bulk acetic acid (singlet at 2.05 ppm and quintet at 2.03 ppm due to residual H in acetic acid-d_4) and an HOD signal at 11.6 ppm from water in the sample (off-scale). This data suggests that not only do the terminal ace-

Table 1
Ligand substitution at molybdenum bi-oxo capped carboxylate trimers.

Attached ligand	Incoming ligand	k^{298K}(s^{-1})	$\Delta H^‡$ (kJ mol^{-1})	$\Delta S^‡$ (J mol^{-1} K^{-1})	Mechanism
η-O_2CCH_3	D_2O	7.2×10^{-6}	126	80	I_D[a]
η-O_2CCH_3	CD_3OD	2.5×10^{-5}	115	52	I_D[a]
η-OH_2	H_2O	5.6×10^{-6}	126	77	I_D[b]
η-OH_2	$C_2O_4^{2-}$	8×10^{-6}	120	85	I_D[b]
η-OH_2	SCN^-	9.4×10^{-6}	141	131	I_D[b]
η-OH_2	CD_3OD	11×10^{-6}	–	–	I_D or D[c]

[a] This work.
[b] Aqueous solutions, Ref. [7].
[c] T = 44.8 °C, neat CD_3OD Ref. [9].

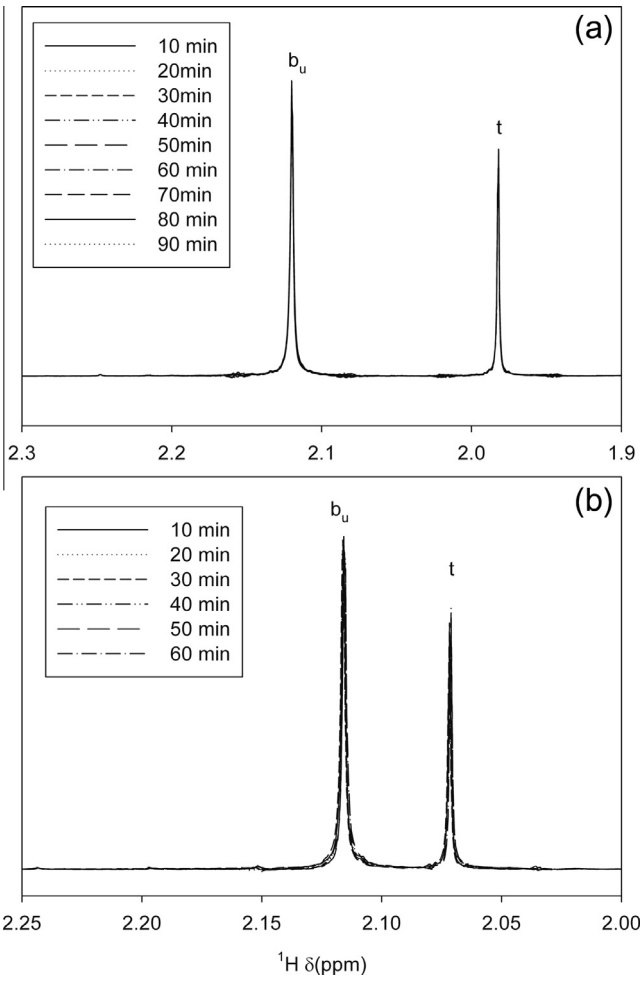

Fig. 3. Substitution reaction run in DMSO-d_6 (a) and DMF-d_7 (b) at $T = 323.0$ K. Bridging acetates (b_u) and ligated acetates (t) are labeled on the spectra. Free acetate appears at 1.83 (DMSO) and 1.89 (DMF) ppm and is not shown on the NMR spectrum. No evidence of reaction was observed for over one hour. The integration of terminal to bridging was 1:2 and remained constant throughout the experiment.

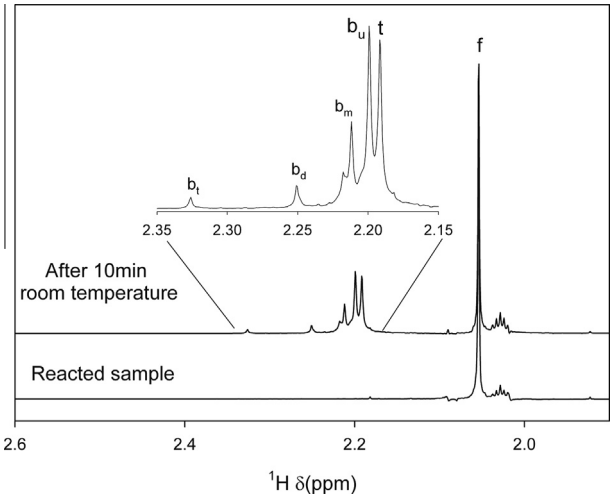

Fig. 4. ^{1}H NMR data for acetate exchange by acetic acid-d_4 ($T = 298.1$ K). After dissolution (top spectrum), signals from the free acetate (2.05 ppm, f), terminal acetates (2.19 ppm, *t*), bridging acetates from substituted species (2.2–2.32 ppm) are observed (b_m, b_d, b_t). The b_m signal, as well as the b_d signal, although not completely resolved, is split into two peaks with a 1:2 ratio due to asymmetry upon substitution. Assignments are based on substituted species observed for rhodium trimers (see Ref. [16]). A signal from HOD is observed at 11.6 ppm but is not shown.

tates exchange quickly with the solvent but the bridging acetates exchange as well. Bridging acetate exchange with acetic acid-d_4 was observed by Noey et al. for an analogous tungsten trimer but at higher temperatures due to the relative inertness of the tungsten complex [12]. No attempts to quantify bridging acetate exchange were made since the focus of the study is to understand the reactivity of terminal acetates.

Kinetic analysis of terminal acetate exchange (Scheme 1) gives an observed rate constant of 3.4×10^{-4} s^{-1} (using Eq. (1)). Because acetic acid-d_4 is the solvent and the back reaction is negligible since acetic acid-d_4 is in excess (described by k'_{obs}), first order kinetics apply. From the temperature dependence of the rates, the $\Delta H^{\ddagger}_{obs}$ and $\Delta S^{\ddagger}_{obs}$ were calculated to be 63 (±12) kJ mol^{-1} and −97 (±40) J mol^{-1} K^{-1}, respectively, and are drastically different than those for acetate substitution by D_2O and methanol-d_4 (Fig. 5). Given the small enthalpy and negative entropy, an obvious pathway to postulate is associative attack at the Mo(IV) metal center (A or I_A). However, considering the number of studies that report dissociative pathways for ligand substitution (see Table 1) and the steric hinderance about the 9-coordinate Mo(IV) ion, an associative pathway seems unlikely.

As a result, acetate exchange at **Mo_3** is thought to be more complex than a simple ligand exchange reaction. Although acetic acid is a weak acid and dissociates less than 0.5% (pK_a acetic acid-d_4, $H_2O/HOD = 4.771$, $[D^+] \sim 1.7 \times 10^{-2}$ M in glacial acetic at 25 °C [17]), our data indicates that acetate exchange is acid catalyzed and likely involves substitution at the ligated acetate. Cotton et al. hypothesized that molybdenum acetates undergo acid-catalyzed hydrolysis reactions similar to organic esters but activation parameters were not measured (0.1 M HCl solution in D_2O, [11]). Ester hydrolysis in the presence of acid typically follows a bimolecular nucleophilic substitution (A_{AC2}) in which a tetrahedral intermediate forms prior to cleavage of the acyl-oxygen bond [18,19]. According to this mechanism, attack of a water molecule at the carbonyl carbon is the rate-determining step [18], which is characterized by a small enthalpy and negative entropy (ethyl acetate hydrolysis: $\Delta H^{\ddagger} = 65$ kJ mol^{-1}; $\Delta S^{\ddagger}$ −26.1 J mol^{-1} K^{-1} [20]). We suggest a similar sequence (Scheme 2) in which rapid pre-equilibrium involving protonation occurs in the first step (Step 1) followed by attack of the carbonyl carbon by an HOD molecule (Rate determining, Step 2). This is then followed by C-O bond cleavage and rapid acetate dissociation (Step 3), which is the step observed by the ^{1}H NMR experiment. Lastly, aqua ligand substitution occurs in which the equilibrium most likely lies to the right given the large concentration of acetic acid-d_4 (Step 4). Although ligand substitution in the final step may be slower than Step 2, substitution in Step 4 cannot be observed by the ^{1}H NMR experiment because the incoming ligand is deuterated and the HOD signal is affected by rapid proton-deuterium exchange with the solvent.

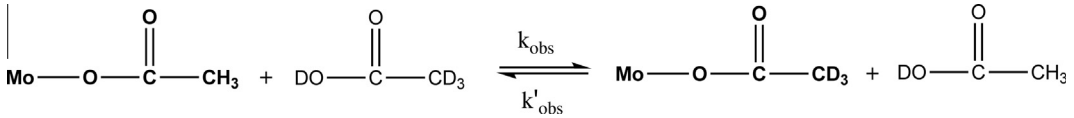

Scheme 1.

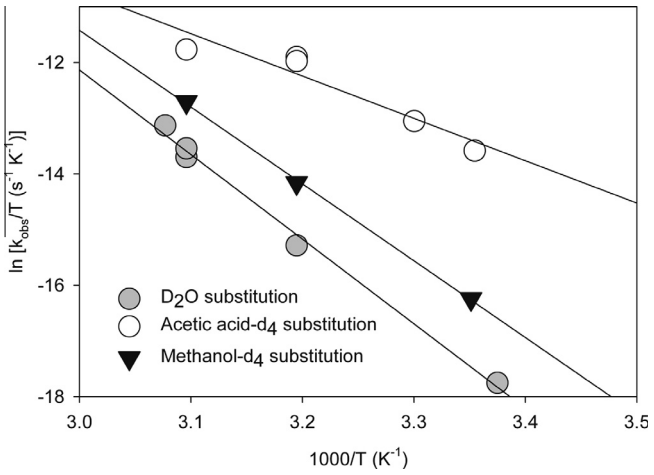

Fig. 5. A plot of $\ln(k_{obs}/T)$ vs. $1/T$. The $\Delta H^{\ddagger}$ and $\Delta S^{\ddagger}$ for substitution by D_2O and methanol-d_4 are highly positive suggesting a dissociative reaction while exchange involving acetic acid-d_4 shows a small $\Delta H^{\ddagger}_{obs}$ and negative $\Delta S^{\ddagger}_{obs}$.

Even though acetate exchange appears to be more complex than a simple ligand exchange reaction, pseudo-first order kinetics still apply Eqs. (3–7). Since Step 2 is considered to be rate-limiting [18], and the back reaction for dissociation (described by k_{-2}) is likely negligible because water is in excess, the rate law takes on the form of Eq. (3), where $\mathbf{Mo_3}^{\nabla}$ refers to the intermediate $\mathbf{Mo_3}$ species with the protonated carbonyl.

$$\text{rate} = k_2[Mo_3^{\nabla}][HOD] \tag{3}$$

The concentration of the $\mathbf{Mo_3}^{\nabla}$ can be expressed in terms of the concentration of the starting $\mathbf{Mo_3}$ complex by taking into consideration the equilibrium constant, K_{eq}, that describes the pre-equilibrium in Step 1 Eq. (4).

$$K_{eq} = \frac{[Mo_3^{\nabla}]}{[Mo_3][D^+]} \tag{4}$$

As a result, the rate of reaction can be expressed in terms of the starting concentration of $\mathbf{Mo_3}$, acid concentration (D^+), and concentration of water. We also include a statistical factor of three to describe three exchange events because each $\mathbf{Mo_3}$ complex has three ligated acetates [21] Eq. (5).

$$\text{rate} = 3k_2K_{eq}[Mo_3][D]^+[HOD] \tag{5}$$

Finally, the concentration terms for acid (D^+) and water (HOD) become components of the observed rate constant because the concentration of acid (1.7×10^{-2} M in glacial acetic at 25 °C [17]) and water, which are the solvent, are in excess relative to $\mathbf{Mo_3}$ (7.0×10^{-4} M) and both are regenerated as products in the proposed mechanism Eqs. (6–7).

$$k_{obs} = 3k_2K_{eq}[D^+][HOD] \tag{6}$$

$$\text{rate} = k_{obs}[Mo_3] \tag{7}$$

Observed rate constants for all reactions are summarized in Table 2.

Given the multi-step nature of the acetate exchange reaction (Scheme 2), it is important to note that our measured parameters are composite values and reflect not only the kinetic pathway but also the first step, protonation equilibrium ($\Delta H^{\ddagger}_{obs} = \Delta H^{\circ} + \Delta H^{\ddagger}$; $\Delta S^{\ddagger}_{obs} = \Delta S^{\circ} + \Delta S^{\ddagger}$, see Supporting information for detailed kinetic analysis). In order avoid any ambiguity, we refer to these parameters as an observed enthalpy and entropy, and denote them as such, $\Delta H^{\ddagger}_{obs}$ and $\Delta S^{\ddagger}_{obs}$.

Even though the measured activation parameters are composite parameters, the main conclusions of our paper still stand. For the acetate ion, the ΔH° of protonation, albeit for the free base, is rather small and negligible (ΔH° = −1.4, −2.74, 0.15 kJ mol^{-1}; T = 25, 40, 45 °C [22–25]). This indicates that its contribution to the observed enthalpy, $\Delta H^{\ddagger}_{obs}$, is minor and within the reported experimental error ($\Delta H^{\ddagger}_{obs}$ = 63 (±12) kJ mol^{-1}). The entropy term for protonation, however, is more significant (ΔS° = 83–88 J mol^{-1} K^{-1} [22–25]). Yet when taken into account as a contributing factor to the composite entropy ($\Delta S^{\ddagger}_{obs}$ = −97 (±40) J mol^{-1} K^{-1}), the magnitude and

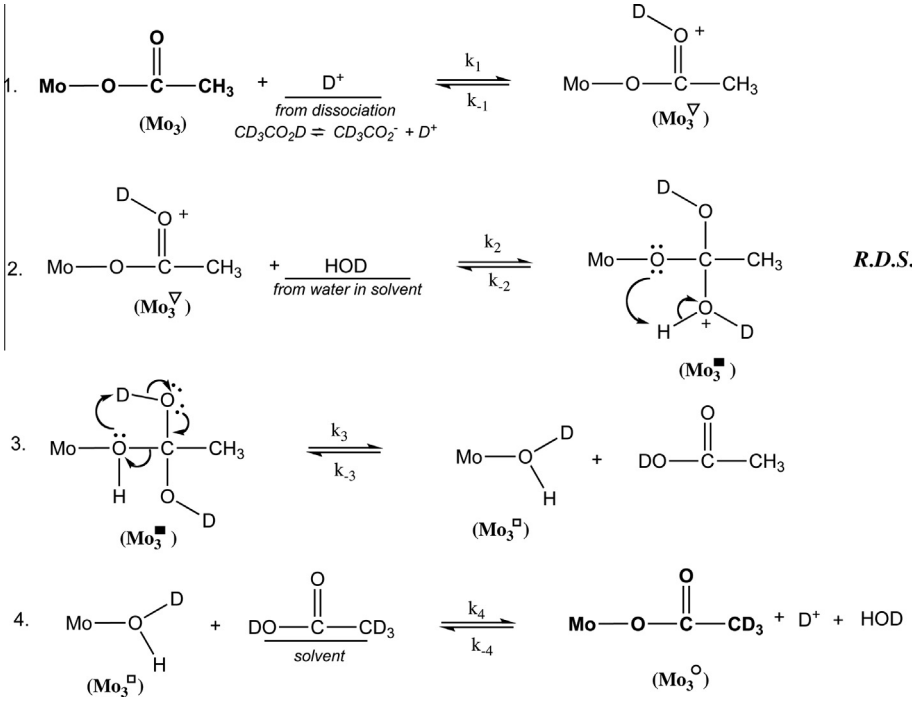

Scheme 2.

Table 2
Terminal acetate substitution at **Mo_3** by polar protic and aprotic solvents.

Solvent	Temperature (K)	k_{obs} (s^{-1})	$\Delta H^{\ddagger}$ (kJ mol^{-1})	$\Delta S^{\ddagger}$ (J mol^{-1} K^{-1})
D_2O	325.0	6.4 (±0.2) × 10^{-4}	126 (±6)	80 (±18)
	323.0	4.2 (±0.5), 3.6(±0.2) × 10^{-4}		
	313.0	7.2 (±0.2) × 10^{-5}		
	296.3	5.8 (±0.4) × 10^{-6}		
Methanol-d_4	323.0	9.7 (±0.4) × 10^{-4}	115 (±3)	52 (±9)
	313.0	2.21 (±0.06) × 10^{-4}		
	298.4	2.6 (±0.2) × 10^{-5}		
Acetic acid-d_4	323.0	2.5 (±0.2) × 10^{-3}	63 (±12)[a]	−97 (±40)[a]
	313.0	2.1 (±0.3), 2.0 (±0.4) × 10^{-3}		
	303.0	6.5 (±0.2) × 10^{-4}		
	298.1	3.70 (±0.09) × 10^{-4}		
DMSO-d_6	323.0	no reaction	–	–
DMF-d_7	323.0	no reaction	–	–

[a] Experimental activation parameters are reported, which include both the activation enthalpy and entropy for protonation.

sign of the true $\Delta S^{\ddagger}$ is even more large and negative ($\Delta S^{\ddagger}$ = −180 J mol^{-1} K^{-1} based on a ΔS° = 83 J mol^{-1} K^{-1}) and so still implies a bimolecular substitution. As a result, the activation parameters presented here, albeit composites, suggest that acetate exchange does not follow a classical ligand exchange pathway, as one might expect, yet is more complicated and most likely involves substitution at the ligated acetate.

Reports of complexation reactions involving substitution at ligands are not uncommon. Although acid-catalyzed hydrolysis reactions are typically carried out in strong acid, complexation reactions involving transition metal complexes in the presence of weak acids such as $HC_2O_4^-$ have been reported before [7,26,27]. For example, Richens proposed a similar pathway for water substitution by $HC_2O_4^-$ at $[Mo_3(\mu_3\text{-}O)_2(\mu\text{-}O_2CCH_3)_6(H_2O)_3]^{2+}$ in acid pH (pH 2.5–3.9) that involved cleavage of the C–O bond rather than Mo–O bond and the activation parameters were similar to the those presented here ($\Delta H^{\ddagger}$ = 76 kJ mol^{-1}, $\Delta S^{\ddagger}$ −67 J mol^{-1} K^{-1}, Ref. [7]).

In summary, we find that acetate substitution by D_2O and methanol-d_4 results in a dissociative activation state based on highly positive activation parameters. Unlike D_2O and methanol-d_4, little to no reaction occurs in DMSO-d_6 and DMF-d_7 most likely because the aprotic solvent is not able to solvate the leaving acetate ligand through hydrogen bonding. The observed enthalpy and entropy terms for acetate exchange are markedly different and support the reaction mechanism originally proposed by Cotton et al. [11] involving hydrolysis of the ligated acetate. The results from this study are insightful and may apply to acid-catalyzed ligand substitutions at other transition metal clusters with terminal carboxylate ligands.

Acknowledgments

This work was supported by the College of Natural Sciences and Mathematics, California State University, Sacramento and the University Enterprises Faculty Awards program. The 500 MHz spectrometer was purchased using grant NSF ARRA-0922676. We would also like to thank undergraduate students Sergio Toscano, Matt Zimmerman and Britainie Ault.

Appendix A. Supplementary material

Supplementary data associated with this article can be found, in the online version, at http://dx.doi.org/10.1016/j.ica.2013.07.054.

References

[1] A. Bino, M. Ardon, I. Maor, M. Kaftory, Z. Dori, J. Am. Chem. Soc. 98 (1976) 7093.
[2] M. Ardon, A. Bino, F.A. Cotton, Z. Dori, M. Kaftory, B.W.S. Kolthammer, M. Kapon, G. Reisner, Inorg. Chem. 20 (1981) 4083.
[3] A. Bino, F.A. Cotton, Z. Dori, B.W.S. Kolthammer, J. Am. Chem. Soc. 103 (1981) 5779.
[4] M. Ardon, A. Bino, F.A. Cotton, Z. Dori, M. Kaftory, Inorg. Chem. 21 (1982) 1912.
[5] K.A. Pineda, J.C. Fettinger, J.R. Houston, Inorg. Chim. Acta 392 (2012) 485.
[6] A. Bino, D. Gibson, Inorg. Chim. Acta 65 (1982) L37.
[7] G. Powell, D.T. Richens, Inorg. Chem. 32 (1993) 4021.
[8] J.R. Houston, D.T. Richens, W.H. Casey, Inorg. Chem. 45 (2006) 7962.
[9] K. Nakata, A. Nagasawa, N. Soyama, Y. Sasaki, T. Ito, Inorg. Chem. 30 (1991) 1575.
[10] F.A. Cotton, Z. Dori, D.O. Marler, W. Schwotzer, Inorg. Chem. 22 (1983) 3104.
[11] A. Birnbaum, F.A. Cotton, Z. Dori, D.O. Marler, G.M. Reisner, W. Schwotzer, M. Shaia, Inorg. Chem. 22 (1983) 2723.
[12] E. Noey, J.C. Curtis, S. Tam, D.M. Pham, E.F. Jones, J. Chem. Educ. 88 (2011) 793.
[13] C.E. Housecroft, A.G. Sharpe, Inorganic Chemistry, third ed., Pearson, England, 2008.
[14] R.G. Wilkins, Kinetics and Mechanism of Reactions of Transition Metal Complexes, second ed., VCH, Weinheim, Germany, 1991.
[15] R.S. Macomber, Modern NMR Spectroscopy, John Wiley and Sons, NY, 1998.
[16] J.R. Houston, M.M. Olmstead, W.H. Casey, Inorg. Chem. 45 (2006) 7799.
[17] M. Paabor, R.G. Bates, R.A. Robinson, J. Phys. Chem. 70 (1966) 540.
[18] C.H. Bamford, C.F.H. Tippe, Comprehensive Chemical Kinetics, Elsevier, vol. 10, Amsterdam, NY, 1972, p. 139.
[19] M.L. Bender, Chem. Rev. 60 (1960) 53.
[20] G. Davies, D.P. Evans, J. Chem. Soc. (1940) 339.
[21] K. Murmann, J. Phys. Chem. 71 (1967) 974.
[22] A.E. Martell, R.M. Smith, Critical Stability Constants, vol. 6, Plenum Press, New York, 1989.
[23] P.L. Zanonato, P. Di Bernardo, A. Bismondo, L. Rao, G.R. Choppin, J. Solution Chem. 30 (2001) 1.
[24] L. Rao, Z. Zhang, P.L. Zanonato, P. Di Bernardo, A. Bismondo, S.B. Clark, Dalton Trans. (2004) 2867.
[25] J. Jiang, L. Rao, P. Di Bernardo, P.L. Zanonato, A. Bismondo, Dalton Trans. (2002) 1832.
[26] C. Andrade, R.B. Jordan, H. Taube, Inorg. Chem. 9 (1970) 711.
[27] P.M. Angus, W.G. Jackson, Inorg. Chim. Acta 287 (1999) 1.